

An Efficient Labelling Approach to Harness Backbone and Side-Chain Protons in ^1H -Detected Solid-State NMR Spectroscopy

Deni Mance, Tessa Sinnige, Mohammed Kaplan, Siddarth Narasimhan, Mark Daniëls, Klaartje Houben, Marc Baldus,* and Markus Weingarth*

Abstract: ^1H -detection can greatly improve spectral sensitivity in biological solid-state NMR (ssNMR), thus allowing the study of larger and more complex proteins. However, the general requirement to perdeuterate proteins critically curtails the potential of ^1H -detection by the loss of aliphatic side-chain protons, which are important probes for protein structure and function. Introduced herein is a labelling scheme for ^1H -detected ssNMR, and it gives high quality spectra for both side-chain and backbone protons, and allows quantitative assignments and aids in probing interresidual contacts. Excellent ^1H resolution in membrane proteins is obtained, the topology and dynamics of an ion channel were studied. This labelling scheme will open new avenues for the study of challenging proteins by ssNMR.

The recent advent of ^1H -detection in biological solid-state NMR (ssNMR) spectroscopy can greatly increase spectral sensitivity,^[1] and thereby bears the potential to critically broaden the scope of ssNMR spectroscopy. The prevailing method to detect protons in solid proteins is perdeuteration, that is, the complete deuteration and subsequent reintroduction of exchangeable protons in protonated buffers. This labelling scheme largely removes line-broadening ^1H – ^1H dipolar couplings and can provide spectra of extremely high quality.^[2] Moreover, it allows automated backbone assignments^[3] and probing contacts between backbone amino protons (H^{N}), which are important to define protein folds.^[4]

However, the absence of aliphatic side-chain protons in perdeuterated proteins curtails the potential of ^1H -detection, given that side chains are important factors for protein structure and function. In addition, the availability of side-chain protons could facilitate the assignment of complex

proteins. In general, to assign side-chain protons and use them for structural studies has remained a major difficulty for ^1H -detected ssNMR spectroscopy. In principle, fully protonated proteins in combination with magic-angle spinning (MAS) frequencies of higher than 100 kHz^[2d] could provide a future avenue to access side-chain protons, as suggested in recent studies with soluble and membrane proteins.^[5] However, it can be envisaged that the residual ^1H linewidths and spectral crowding will remain a challenge for larger proteins. Moreover, for proteins such as membrane proteins with a substantial inhomogeneous contribution to the ^1H linewidth, MAS frequencies higher than 100 kHz may not compensate for the sensitivity loss resulting from comparably small sample volumes. Excellent resolution and assignments of aliphatic protons have been reported with residual adjoining protonation (RAP), which relies on the random incorporation of protons into a deuterated protein matrix.^[6] Moreover, approaches such as ILV, proton cloud, or SAIL labelling can be used to probe contacts between side-chain protons of specific types of amino acids.^[7] Yet, such approaches employ isolated labels which may be very difficult to assign de novo and only give access to a selection of side-chain protons. To assign side-chain protons and exploit them for structural studies, even in larger proteins, a labelling scheme which 1) provides a high global ^1H density and 2) mitigates spectral crowding nonetheless, could be very advantageous. Thus we explored “fractional deuteration” in ^1H -detected ssNMR spectroscopy. This labelling scheme, based on protonated ^{13}C -glucose and D_2O in the growth medium, was previously proposed in solution NMR spectroscopy as an alternative to ILV labelling and in ^{13}C -detected ssNMR spectroscopy for spectral editing.^[8] These studies reported that certain carbon atoms, such as $\text{C}\alpha$, are highly deuterated in fractionally deuterated proteins, while many side-chain carbon atoms retain sizeable ^1H levels.

Herein we demonstrate that fractional deuteration provides access to well-resolved H^{N} and side-chain protons of virtually all residues in one sample, and allows assignment and use of these protons for structural studies. Importantly, even though our approach works at much higher ^1H levels, we observe an excellent resolution (0.07 ppm) for the H^{N} protons in the fractionally deuterated (FD) membrane-embedded K^+ channel KcsA, and it rivals the resolution in the perdeuterated channel. We outline our approach on ubiquitin and then use it to study KcsA, including its membrane topology and dynamics, as well as important channel–water interactions.

Figure 1 shows ^1H -detected two-dimensional (2D) CH and NH spectra of FD [^{13}C , ^{15}N]-ubiquitin in aqueous (100% H_2O) buffers, acquired at 52 kHz MAS and 800 MHz ^1H -

[*] D. Mance, Dr. T. Sinnige,^[†] M. Kaplan, S. Narasimhan, M. Daniëls, Dr. K. Houben, Prof. M. Baldus, Dr. M. Weingarth
 NMR Spectroscopy, Bijvoet Center for Biomolecular Research,
 Department of Chemistry, Faculty of Science, Utrecht University
 Padualaan 8, 3584 CH Utrecht (The Netherlands)
 E-mail: M.Baldus@uu.nl
 M.H.Weingarth@uu.nl

[†] Present address: Department of Chemistry, University of Cambridge
 Lensfield Road, Cambridge CB2 1EW (UK)

Supporting information for this article is available on the WWW
 under <http://dx.doi.org/10.1002/anie.201509170>.

© 2015 The Authors. Published by Wiley-VCH Verlag GmbH & Co. KGaA. This is an open access article under the terms of the Creative Commons Attribution Non-Commercial NoDerivs License, which permits use and distribution in any medium, provided the original work is properly cited, the use is non-commercial and no modifications or adaptations are made.

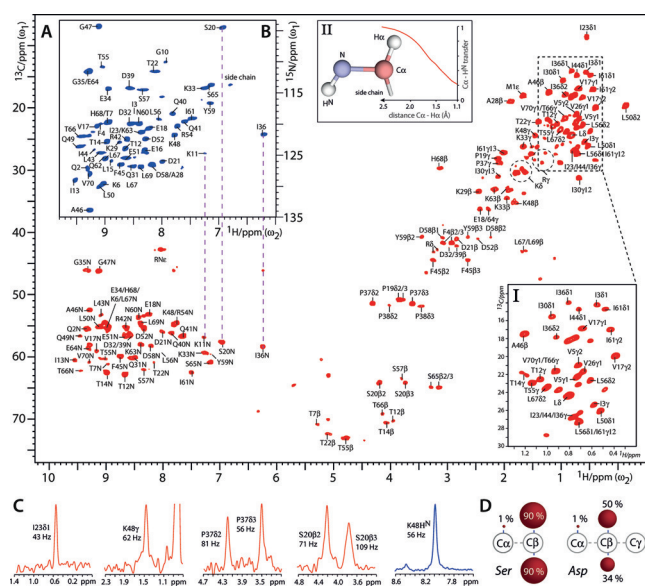


Figure 1. ^1H -detected ssNMR experiments in FD ubiquitin. A) 2D CH spectrum (in red). Box I shows an expansion of the methyl region. Box II shows simulations of the influence of $\text{C}\alpha\text{H}\alpha$ dipolar couplings on the CP transfer from $\text{C}\alpha$ to H^{N} . B) 2D NH spectrum (blue). C) Cross-sections from the 2D CH (in red) and NH (blue) experiments. D) Examples of the protonation pattern in FD amino acids. See Table S1 for the complete list. Red spheres illustrate the ^1H level at a given ^{13}C .

frequency using MISSISSIPPI water suppression^[9] and low-power PISSARRO decoupling.^[10] These spectra are of remarkable quality and feature a resolution as high as 0.05 and 0.07 ppm for aliphatic and exchangeable protons, respectively. The absence of $\text{C}\alpha\text{H}\alpha$ correlations, which typically appear around $\delta_{^{13}\text{C}} = 50\text{--}65$ ppm and $\delta_{^1\text{H}} = 3.0\text{--}5.0$ ppm, is readily visible in the CH spectrum. A quantitative analysis using solution NMR spectroscopy (see section S1 in the Supporting Information) revealed, next to the absence of $\text{H}\alpha$ protons ($<2\%$ population), an interesting pattern of ^1H depletion for the side chains in FD ubiquitin (see Figure 1D and Table S1). The pyruvate-derived branched-chain amino acids (Ile, Leu, Val) exhibit very low ($\leq 5\%$) ^1H levels at the $\text{C}\beta$ -position, which is the same for the amino acids (Arg, Gln, Glu, Pro) derived from α -ketoglutarate ($\leq 8\%$). Amino acids that follow other pathways (such as Asn, Asp, His, Lys, Ser, Thr), however, retain much higher ^1H levels (30–45%; 90% for Ser) at $\text{C}\beta$, with slightly reduced values for aromatic amino acids (Phe, Tyr). Most other carbon atoms, further away from the backbone, feature equally high ^1H levels. Our data are in good agreement with the original solution NMR study, which also provides detailed biochemical explanations.^[8a] Hence, many sites remain robustly protonated in FD proteins, yet feature a narrow ^1H linewidth because the ^1H network is, on average, starkly diluted. However, we like to emphasize that the local and global ^1H density in FD proteins are much higher than those in RAP-labelled proteins.^[6] Broadening effects resulting from methylene isotopomers were not observed, probably because CH_2 signals are broadened beyond detection. Methyl groups showed slight oval line-shapes because of isotopomers, but they did not significantly

compromise the ^1H resolution (0.05–0.08 ppm), presumably because CH_3 signals are broader and less abundant than either CHD_2 or CH_2D signals (see Box I in Figure 1A and Figure S2). Prominent features of the CH spectrum of FD ubiquitin are the unusually intense $\text{C}\alpha\text{H}^{\text{N}}$ signals. As it can be readily shown with simulations (see Box II in Figure 1A and section S2), this beneficial effect is caused by the absence of $\text{H}\alpha$ protons in FD proteins.^[11]

In Figure 2A we show assignments in FD ubiquitin, and they are based on dipolar transfer. Acquisition details can be found in section S2. Backbone connectivities were established with three-dimensional (3D) $\text{C}\alpha\text{NH}$, $\text{C}\alpha(\text{CO})\text{NH}$, and CCH

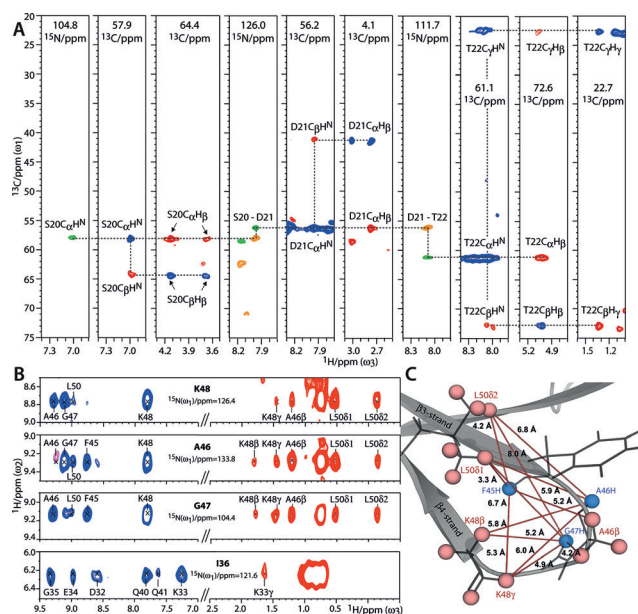


Figure 2. ^1H -detected assignments and structural studies in FD ubiquitin at 52 kHz MAS. A) Walk through S20–T22 (see section S3 for further walks). Signals from 3D $\text{C}\alpha\text{NH}$ (green), $\text{C}\alpha(\text{CO})\text{NH}$ (orange), and CCH (blue for positive; red for negative signals) experiments, are color-coded. B) Strips from a 3D NHH experiment. $\text{H}^{\text{N}}\text{--H}^{\text{N}}$ contacts and inter-residual contacts between H^{N} and side-chain protons are shown in blue and red, respectively. C) Illustration of the contacts shown in (B). $\text{H}^{\text{N}}\text{--H}^{\text{N}}$ contacts are not shown for clarity.

experiments. In the 3D $\text{C}\alpha(\text{CO})\text{NH}$, $\text{C}\alpha$ polarization was prepared by a selective CP step (see Figure S4).^[2g, 12] These experiments were sufficient for backbone assignments, given that extensive chemical-shift data are available for ubiquitin.^[13] Side-chain assignments were performed with a 3D CCH experiment which included a $^{13}\text{C}\text{--}^{13}\text{C}$ DREAM^[14] double-quantum mixing block, optimized for one-bond transfer. Importantly, the efficient transfer from $\text{C}\alpha$ to H^{N} in the CCH experiments, and hence the presence of intense $\text{C}\alpha\text{C}\beta\text{H}\beta$ and $\text{C}\beta\text{C}\alpha\text{H}^{\text{N}}$ correlations, allow the use of H^{N} as anchors to connect backbone and side chains, thereby greatly facilitating the assignment process. Moreover, the assignments of side-chain types are greatly simplified by the pattern of robustly protonated and deprotonated $\text{C}\beta$ sites (see Table S1). $\text{C}\alpha\text{C}\beta\text{H}\beta$ correlations were only detectable for residues with $\text{H}\beta$ levels of greater than 20%, which much

reduced ambiguity. In total, we could assign the H β signals for 24 of the 28 residues with ^1H levels of greater than 20% (ignoring the mobile residues M1, T9, L27).^[13b] Other inaccessible H β signals were from surface-exposed, and likely mobile, residues (K11, N25, N60). Additional side-chain protons such as the H γ of Thr and Lys could also be readily assigned. To identify the methyl groups of Leu, Ile, Val, and Met, we resorted to published assignments.^[2d,13a] Such side-chain protons could also be assigned with longer ^{13}C - ^{13}C mixing.

Thanks to the high ^1H density and resolution in FD proteins, the side-chain assignments can be readily exploited for structural studies, which are shown in Figures 2B and C. We carried out a 3D NHH experiment with 1.5 ms ^1H - ^1H DREAM mixing,^[2d,7a] in which we detected backbone-backbone H $^{\text{N}}$ -H $^{\text{N}}$ contacts, as well as backbone-side chain contacts between H $^{\text{N}}$ and aliphatic protons. Next to a large number of H $^{\text{N}}$ -H $^{\text{N}}$ contacts, many interresidual backbone-side chain contacts, of up to an 8 Å distance, could be assigned or identified (based on the X-ray structure PDB: 1UBQ). These contacts demonstrate that the high ^1H density in FD proteins does not impede long-distance magnetization transfer. Unambiguous medium- and long-range ^1H - ^1H contacts involved methyl groups and also methylene groups such as the C β HD and C γ HD groups of Lys residues. Especially the latter contacts are noteworthy, since they are complementary to ILV labelling.

In Figures 3 and 4, we show the potential of ^1H -detection in more complex FD proteins using the K $^+$ channel KcsA, a well-accepted model for ion-channel gating,^[15] as an example. FD [^{13}C , ^{15}N]-KcsA in the closed-conductive state was reconstituted in *E. coli* lipids and aqueous (100% H $_2\text{O}$) buffers. Further details of the sample preparation are given in section S5. We acquired dipolar-based 2D NH and CH spectra of very high quality (Figure 3A and Figure 4A), featuring a resolution as high as 0.06 and 0.07 ppm for aliphatic and exchangeable protons, respectively. Remarkably, the H $^{\text{N}}$ resolution in FD KcsA is comparable to perdeuterated KcsA^[5c] (see Figure S11) and the perdeuterated membrane protein OmpG^[3a] (0.13–0.18 ppm). This resolution strongly suggests that the availability of side-chain protons in many FD membrane proteins comes at either very low or no cost at fast (>50 kHz) MAS, because the residual ^1H linewidth is dominated by inhomogeneous contributions. Hence, fractional deuteration is highly advantageous for ^1H -detection in non-microcrystalline proteins.

FD KcsA was grown in D $_2\text{O}$ and only water-exposed residues are visible in the NH spectrum, which we used to study the membrane topology.^[2c,5c] Intriguingly, the NH spectrum showed only around 25 signals, while KcsA features about 70 water-accessible residues, which, in particular, comprise the extracellular outer vestibule (residues 51–64 and 80–86) and the cytoplasmic domain (CPD; residues 118–160). To understand the composition of the NH spectrum, we performed 3D CaNH, 3D Ca(CO)NH, 3D NHH, 2D CH, and 2D C(C)H experiments (see section S3 for a detailed discussion of the assignments), supported by ^{13}C - and ^{15}N -chemical-shift data.^[15c,d] We validated our sequential assignments by H $^{\text{N}}$ -H $^{\text{N}}$ contacts which we observed in a 3D NHH

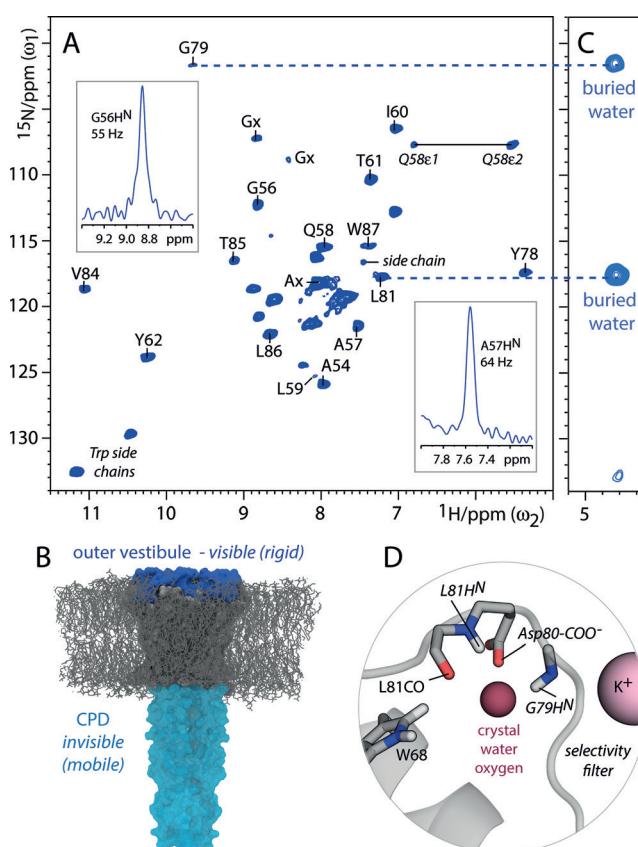


Figure 3. ^1H -detected studies with FD KcsA (closed-conductive). A) Dipolar-based 2D NH spectrum measured at 52 kHz MAS. B) The CPD is absent in this spectrum because of dynamics. C) Section of a 2D N(H)H spectrum using 0.75 ms ^1H - ^1H DREAM mixing showing transfer of G79H $^{\text{N}}$ and L81H $^{\text{N}}$ to buried water behind the selectivity filter. The signals have negative intensity. D) Illustration of a KcsA structure (PDB: 1K4C).

experiment (see Figure S7). Moreover, by using a slightly longer ^{13}C to ^1H CP contact time (700 μs), we obtained many CaH $^{\text{N}+1}$ contacts in the 2D CH, which also allowed validation of sequential assignments (see Figure S8). Altogether, we could assign about 70% of the H $^{\text{N}}$ signals, which all belonged to the outer vestibule, thus demonstrating that the CPD is too dynamic for dipolar transfer (Figure 3B). Note that we did not observe marked sensitivity with scalar transfer, thus implying that CPD dynamics in lipid membranes are relatively slow (μs to ms). We also did not observe the CPD in open-inactivated KcsA (see Figure S10), where the CPD helices are loosely structured. The latter result, thus, excludes the possibility that the CPD is invisible in the 2D NH of the closed-conductive channel (Figure 3a) because of tight packing of CPD helices, which might possibly interfere with the reintroduction of protons. This finding is noteworthy given that the conformational flexibility of the CPD is important for KcsA activation gating.^[15b] Furthermore, in Figures 3C and D we used our ^1H assignments to study buried water behind the conductive selectivity filter, as it is important for the gating mode.^[5c,15a] How this water is bound is not directly accessible in KcsA X-ray structures, since protons are not resolved. By transferring magnetization

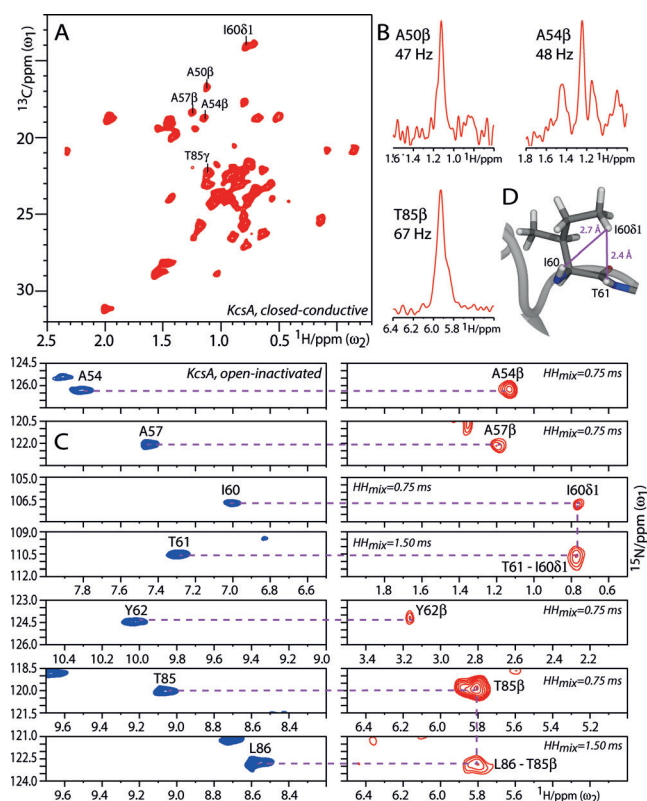


Figure 4. ^1H -detection of side chains in FD KcsA. A) Section of a 2D CH spectrum measured at 58 kHz MAS with closed-conductive KcsA. Cross-sections are shown in (B). C) Left: Sections from a 2D NH spectrum (blue); right: Sections from a 2D N(H)H spectrum (red) acquired with open-inactivated KcsA. D) The contact T61H $^{\text{N}}$ -I60H δ 1 is illustrated in the snapshot of an MD simulation. See section S3 for additional side-chain assignments.

from H $^{\text{N}}$ to buried water in 2D and 3D NHH experiments (see Figure S12) using DREAM mixing, we see that G79H $^{\text{N}}$ and L81H $^{\text{N}}$ contact buried water, thus strongly suggesting that both coordinate the water oxygen atom while water protons contact the nearby Asp80-COO $^-$ group and L81CO.

The assignment of the spectrum in Figure 3 A was greatly simplified by the availability of side-chain protons. As described for FD ubiquitin, we connected side-chain and backbone information through H $^{\text{N}}$ anchor protons (see Figure 4C and Figure S8). We thus assigned de novo side chains by a 2D C(C)H experiment as well as 2D and 3D NHH experiments which included a short (750 μs) ^1H - ^1H DREAM transfer. Note that longer (1.5 ms) ^1H - ^1H mixing also allowed structural studies of side-chain protons (Figure 4C,D). Only residues with H β levels of greater than 20% showed (H $^{\text{N}}$)CaH β and NH $^{\text{N}}$ H β correlations in these experiments, and we readily assigned residues such as A54, A57, T61, Y62, and T85.

In conclusion, we have introduced a labelling approach for ^1H -detected ssNMR spectroscopy, which provides far-reaching access to very well resolved backbone and side-chain protons. Most importantly, for non-microcrystalline samples, our method greatly expands the power of the formidable perdeuteration approach without sacrificing much, if any, ^1H resolution. We believe that our approach, which also avoids

the use of expensive deuterated glucose, will significantly increase the impact of solid-state NMR spectroscopy, especially for membrane proteins or peptide assemblies such as fibrils, which usually cannot be obtained as microcrystalline preparations.

Acknowledgments

We acknowledge financial support from the NWO (700.26.121, 700.10.443, 722.012.002, and 723.014.003).

Keywords: ion channels · membrane proteins · proton detection · side-chain protons · solid-state NMR spectroscopy

How to cite: *Angew. Chem. Int. Ed.* **2015**, *54*, 15799–15803
Angew. Chem. **2015**, *127*, 16025–16029

- [1] Y. Ishii, R. Tycko, *J. Magn. Reson.* **2000**, *142*, 199–204.
- [2] a) V. Chevelkov, K. Rehbein, A. Diehl, B. Reif, *Angew. Chem. Int. Ed.* **2006**, *45*, 3878–3881; *Angew. Chem.* **2006**, *118*, 3963–3966; b) R. Linser, M. Dasari, M. Hiller, V. Higman, U. Fink, J. M. Lopez del Amo, S. Markovic, L. Handel, B. Kessler, P. Schmieder, D. Oesterheld, H. Oschkinat, B. Reif, *Angew. Chem. Int. Ed.* **2011**, *50*, 4508–4512; *Angew. Chem.* **2011**, *123*, 4601–4605; c) L. Shi, I. Kawamura, K. H. Jung, L. S. Brown, V. Ladizhansky, *Angew. Chem. Int. Ed.* **2011**, *50*, 1302–1305; *Angew. Chem.* **2011**, *123*, 1338–1341; d) V. Agarwal, S. Penzel, K. Szekely, R. Cadalbert, E. Testori, A. Oss, J. Past, A. Samoson, M. Ernst, A. Bockmann, B. H. Meier, *Angew. Chem. Int. Ed.* **2014**, *53*, 12253–12256; *Angew. Chem.* **2014**, *126*, 12450–12453; e) J. M. Lamley, D. Iuga, C. Oster, H. J. Sass, M. Rogowski, A. Oss, J. Past, A. Reinhold, S. Grzesiek, A. Samoson, J. R. Lewandowski, *J. Am. Chem. Soc.* **2014**, *136*, 16800–16806; f) P. Schanda, S. Triboulet, C. Laguri, C. M. Bougault, I. Ayala, M. Callon, M. Arthur, J. P. Simorre, *J. Am. Chem. Soc.* **2014**, *136*, 17852–17860; g) V. Chevelkov, B. Habenstein, A. Loquet, K. Giller, S. Becker, A. Lange, *J. Magn. Reson.* **2014**, *242*, 180–188.
- [3] a) E. Barbet-Massin, A. J. Pell, J. S. Retel, L. B. Andreas, K. Jaudzems, W. T. Franks, A. J. Nieuwkoop, M. Hiller, V. Higman, P. Guerry, A. Bertarello, M. J. Knight, M. Felletti, T. Le Marchand, S. Kotelovica, I. Akopjana, K. Tars, M. Stoppini, V. Bellotti, M. Bolognesi, S. Ricagno, J. J. Chou, R. G. Griffin, H. Oschkinat, A. Lesage, L. Emsley, T. Herrmann, G. Pintacuda, *J. Am. Chem. Soc.* **2014**, *136*, 12489–12497; b) S. Q. Xiang, V. Chevelkov, S. Becker, A. Lange, *J. Biomol. NMR* **2014**, *60*, 85–90.
- [4] a) R. Linser, B. Bardiaux, V. Higman, U. Fink, B. Reif, *J. Am. Chem. Soc.* **2011**, *133*, 5905–5912; b) M. J. Knight, A. L. Webber, A. J. Pell, P. Guerry, E. Barbet-Massin, I. Bertini, I. C. Felli, L. Gonnelli, R. Pierattelli, L. Emsley, A. Lesage, T. Herrmann, G. Pintacuda, *Angew. Chem. Int. Ed.* **2011**, *50*, 11697–11701; *Angew. Chem.* **2011**, *123*, 11901–11905.
- [5] a) D. H. Zhou, G. Shah, M. Cormos, C. Mullen, D. Sandoz, C. M. Rienstra, *J. Am. Chem. Soc.* **2007**, *129*, 11791–11801; b) A. Marchetti, S. Jehle, M. Felletti, M. J. Knight, Y. Wang, Z. Q. Xu, A. Y. Park, G. Otting, A. Lesage, L. Emsley, N. E. Dixon, G. Pintacuda, *Angew. Chem. Int. Ed.* **2012**, *51*, 10756–10759; *Angew. Chem.* **2012**, *124*, 10914–10917; c) M. Weingarh, E. A. van der Crujisen, J. Ostmeier, S. Lievestro, B. Roux, M. Baldus, *J. Am. Chem. Soc.* **2014**, *136*, 2000–2007; d) S. Wang, S. Parthasarathy, Y. Xiao, Y. Nishiyama, F. Long, I. Matsuda, Y. Endo, T. Nemoto, K. Yamauchi, T. Asakura, M. Takeda, T.

- Terauchi, M. Kainosho, Y. Ishii, *Chem. Commun.* **2015**, *51*, 15055–15058.
- [6] S. Asami, P. Schmieder, B. Reif, *J. Am. Chem. Soc.* **2010**, *132*, 15133–15135.
- [7] a) M. Huber, S. Hiller, P. Schanda, M. Ernst, A. Bockmann, R. Verel, B. H. Meier, *ChemPhysChem* **2011**, *12*, 915–918; b) T. Sinnige, M. Daniels, M. Baldus, M. Weingarth, *J. Am. Chem. Soc.* **2014**, *136*, 4452–4455; c) S. Wang, S. Parthasarathy, Y. Nishiyama, Y. Endo, T. Nemoto, K. Yamauchi, T. Asakura, M. Takeda, T. Terauchi, M. Kainosho, Y. Ishii, *PLoS one* **2015**, *10*, e0122714.
- [8] a) M. K. Rosen, K. H. Gardner, R. C. Willis, W. E. Parris, T. Pawson, L. E. Kay, *J. Mol. Biol.* **1996**, *263*, 627–636; b) R. Otten, B. Chu, K. D. Krewulak, H. J. Vogel, F. A. Mulder, *J. Am. Chem. Soc.* **2010**, *132*, 2952–2960; c) D. Nand, A. Cukkemane, S. Becker, M. Baldus, *J. Biomol. NMR* **2012**, *52*, 91–101.
- [9] D. H. Zhou, C. M. Rienstra, *J. Magn. Reson.* **2008**, *192*, 167–172.
- [10] M. Weingarth, G. Bodenhausen, P. Tekely, *J. Magn. Reson.* **2009**, *199*, 238–241.
- [11] M. J. Bayro, M. Huber, R. Ramachandran, T. C. Davenport, B. H. Meier, M. Ernst, R. G. Griffin, *J. Chem. Phys.* **2009**, *130*, 114506.
- [12] M. Baldus, A. T. Petkova, J. Herzfeld, R. G. Griffin, *Mol. Phys.* **1998**, *95*, 1197–1207.
- [13] a) M. Schubert, T. Manolikas, M. Rogowski, B. H. Meier, *J. Biomol. NMR* **2006**, *35*, 167–173; b) P. Schanda, B. H. Meier, M. Ernst, *J. Am. Chem. Soc.* **2010**, *132*, 15957–15967.
- [14] R. Verel, M. Baldus, M. Ernst, B. H. Meier, *Chem. Phys. Lett.* **1998**, *287*, 421–428.
- [15] a) J. Ostmeier, S. Chakrapani, A. C. Pan, E. Perozo, B. Roux, *Nature* **2013**, *501*, 121–124; b) S. Uysal, L. G. Cuello, D. M. Cortes, S. Koide, A. A. Kossiakoff, E. Perozo, *Proc. Natl. Acad. Sci. USA* **2011**, *108*, 11896–11899; c) E. A. van der Crujisen, D. Nand, M. Weingarth, A. Prokofyev, S. Hornig, A. A. Cukkemane, A. M. Bonvin, S. Becker, R. E. Hulse, E. Perozo, O. Pongs, M. Baldus, *Proc. Natl. Acad. Sci. USA* **2013**, *110*, 13008–13013; d) B. J. Wylie, M. P. Bhate, A. E. McDermott, *Proc. Natl. Acad. Sci. USA* **2014**, *111*, 185–190.

Received: September 30, 2015

Published online: November 11, 2015